APAMI2020 General Oral Presentation Session | APAMI 2020 | General Oral Presentation Session
Artificial Intelligence in Healthcare and Clinical Practice (2)
Mon. Nov 23, 2020 9:00 AM - 10:10 AM Room E-1 (Congress center 5F - Conference Room 52)

[AP3-E1-1-02] An Application of Heterogeneous Mixture Learning for Mild Cognitive Impairment Subtyping

*Masataka Kikuchi[1], Kaori Kobayashi[1,2], Kensaku Kasuga[3], Akinori Miyashita[3], Takeshi Ikeuchi[3], Eiji Yumoto[4], Yasuto Fushimi[2], Toshihiro Takeda[5], Shirou Manabe[5], Kenichi Kamijo[2], Yasushi Matsumura[5] （1. Department of Genome Informatics, Graduate School of Medicine, Osaka University, Japan, 2. Medical Solutions Division, NEC Corporation, Japan, 3. Department of Molecular Genetics, Brain Research Institute, Niigata University, Japan, 4. Biometrics Research Laboratories, NEC Corporation, Japan, 5. Department of Medical Informatics, Graduate School of Medicine, Osaka University, Japan）

Keywords: Alzheimer Disease, Mild Cognitive Impairment, Decision Trees

Mild cognitive impairment (MCI) is known as a group at high risk of conversion to dementia, including Alzheimer's disease (AD). Individuals with MCI show heterogeneity in patterns of pathology, and do not always convert to AD. Detailed subtyping for MCI and accurate prediction of the patients who convert to AD may allow for new trial designs and may enable evaluation of the efficacy of a drug with a small number of patients during clinical trials. In this study, we applied the heterogeneous mixture learning (HML) method to identify subtypes of MCI. As a result, we identified eight subtypes of MCI using the HML approach and categorized into three groups in terms of AD conversion. The identification of these subtypes revealed varying conversion rates to AD, as well as differing levels of biological features.

An Application of Heterogeneous Mixture Learning for Mild Cognitive Impairment Subtyping

Masataka Kikuchi[a], Kaori Kobayashi[a,b], Kensaku Kasuga[c], Akinori Miyashita[c], Takeshi Ikeuchi[c], Eiji Yumoto[d], Yasuto Fushimi[b], Toshihiro Takeda[e], Shirou Manabe[e], for the Alzheimer's Disease Neuroimaging Initiative, Kenichi Kamijo[b], Yasushi Matsumura[e]

[a] *Department of Genome Informatics, Graduate School of Medicine, Osaka University, Japan*
[b] *Medical Solutions Division, NEC Corporation, Japan*
[c] *Department of Molecular Genetics, Brain Research Institute, Niigata University, Japan*
[d] *Biometrics Research Laboratories, NEC Corporation, Japan*
[e] *Department of Medical Informatics, Graduate School of Medicine, Osaka University, Japan*

Abstract

Mild cognitive impairment (MCI) is known as a group at high risk of conversion to dementia, including Alzheimer's disease (AD). Individuals with MCI show heterogeneity in patterns of pathology, and do not always convert to AD. Detailed subtyping for MCI and accurate prediction of the patients who convert to AD may allow for new trial designs and may enable evaluation of the efficacy of a drug with a small number of patients during clinical trials. In this study, we applied the heterogeneous mixture learning (HML) method to identify subtypes of MCI. As a result, we identified eight subtypes of MCI using the HML approach and categorized into three groups in terms of AD conversion. The identification of these subtypes revealed varying conversion rates to AD, as well as differing levels of biological features.

Keywords:

Alzheimer Disease, Mild Cognitive Impairment, Decision Trees

Introduction

Worldwide, 46.8 million people are affected by dementia, including Alzheimer's disease (AD), which is characterized by the accumulation of amyloid-beta (Aβ) protein and tau protein [1]. Overcoming dementia is an urgent issue because the number of affected individuals is increasing.

Experimental drugs for AD have failed to prevent or slow cognitive decline in people with AD in clinical trials or have shown adverse effects [2]. Although those drugs did not demonstrate excellent clinical efficacy in patients in late-stage AD, they can potentially act effectively in the treatment of patients in early-stage AD or mild cognitive impairment (MCI). However, individuals with MCI show heterogeneity in patterns of pathology, and patients with MCI do not always convert to AD. Detailed subtyping for MCI and accurate prediction of the patients who convert to AD may allow for new trial designs and may enable evaluation of the efficacy of a drug with a small number of patients during clinical trials.

MCI has been classified into four subtypes by clinical diagnosis [3]. This classification divides MCI patients into amnestic or non-amnestic MCI, followed by further division into a group that presents a single impairment in the cognitive domain (single domain) or another group that shows multiple impairments (multiple domain). In particular, amnestic MCI, regardless of single or multiple domain impairments, converts to dementia, mainly AD, at a rate of 10% to 15% per year [4]. Recent studies based on neuropsychological tests also identified some subtypes of MCI [5,6]. The clinical diagnoses and neuropsychological tests often include subjective factors. In addition to the subjective factors, assessment of objective factors such as brain imaging data, biomarker data, and genomic data may offer subtyping of MCI that reflects a more precise conversion rate to AD.

In this study, we applied the heterogeneous mixture learning (HML) method to identify subtypes of MCI. HML divides individuals into similar groups based on various datasets obtained from individuals and generates appropriate predictive models for each group (e.g., whether an individual as input data is a patient with AD or a healthy individual). We characterized the subtypes of MCI identified by HML and examined conversion to AD for each subtype over a given period.

Materials and Methods

Heterogeneous mixture learning

We applied HML to obtain a decision tree for MCI subtyping. HML is a type of hierarchical mixture of expert model [7] that integrate multiple learners using a decision tree. HML divides individuals into similar groups based on various datasets of the individuals and generates appropriate predictive models for each group. As mentioned below, HML simultaneously estimates the parameters for a decision tree and the prediction models using the expectation–maximization (EM) algorithm. Using HML has several advantages: (1) The decision tree facilitates understanding of how individuals are classified into their subtypes. (2) The estimated weight parameters indicate the contribution of each variable to the prediction.

Decision tree

We have observation data $x^N = x^{(1)}, \ldots, x^{(N)}$, where $x^{(n)} \in \mathbb{R}^D$, N is the number of individuals, and D is the number of dimensions in x. A decision tree is composed of the gating nodes as non-leaf nodes and the expert nodes as leaf nodes (Figure 1). The i-th gating node g_i assigns an individual as input data $x^{(n)}$ to an appropriate expert node for prediction based on a rule $x[\gamma_i] < t_i$, where γ_i is the index of variables of x in a gating node

g_i, and t_i is a threshold in a gating node g_i. A binary logistic regression model is used in the expert nodes. The prediction model in the j-th expert node is presented as the following equation:

$$p(y|x, \varphi_j) = \frac{1}{1 + exp(-\varphi_j^T x)}.$$

Let us denote the regression target as $y^N = y^{(1)}, \ldots, y^{(N)}$, where $y^{(n)}$ corresponds to $x^{(n)}$, and φ_j indicates a vector of weight parameters in the j-th expert node.

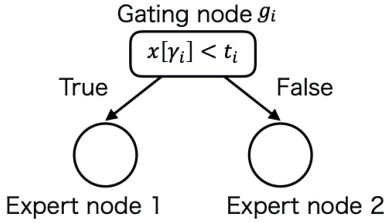

Figure 1- An example of a decision tree

Estimation of parameters by EM-like iterative optimization

To obtain a decision tree model, we needed the parameters for the gating nodes (*i.e.*, g_i, γ_i, and t_i) and the expert nodes (*i.e.*, φ). These parameters were estimated by EM-like iterative optimization. HML automatically selects an optimal decision tree and optimal model parameters to maximize a factorized information criterion [8]. We first set the tree depth d. The maximum number of expert nodes is 2^d since a decision tree is composed of binary trees. The estimation of parameters by EM-like iterative optimization is shown in Algorithm 1, where superscript (k) denote the k-th step, q is an evaluation function, and ζ is a latent variable (see [8] for a detailed description of these steps). q function has regularization effect, avoiding overfitting by some biases in the dataset. In the process of EM-like iterative optimization, the expert nodes with low predictive power are pruned from the decision tree, resulting in a more appropriate tree structure (line 4 in Algorithm 1).

Algorithm 1 Estimation of parameters by EM-like iterative optimization

Input: x^N, y^N
Output: g^*, γ^*, t^*, and ϕ^*
1: Initialization
2: **while** Untile Convergence **do**
3: Update $q^{(k)}(\zeta^{(N)})$ (E-step)
4: Eliminate experts with $\sum_{n=1}^{N} q_j^{(n,k)} < 0.01N$
5: Update $g_i^{(k)}$, $\gamma_i^{(k)}$, $t_i^{(k)}$, and $\phi_j^{(k)}$ (M-step)
6: $k = k + 1$
7: **end while**
8: **return** $g^* = g^{(k)}$, $\gamma^* = \gamma^{(k)}$, $t^* = t^{(k)}$, and $\phi^* = \phi^{(k)}$

Condition setting

We set the tree depth d from three to six. The EM iterative optimization converges to a local optimum depending on an initial value and is not guaranteed to converge to the global optimum. To avoid a local optimum, we performed 30 iterations with different initial values at each depth. We adopted the decision tree with the best accuracy.

Dataset

Data used in this study were obtained from the Alzheimer's Disease Neuroimaging Initiative (ADNI) [9]. The ADNI was launched in 2003 as a public-private partnership led by Principal Investigator Michael W. Weiner, MD. The primary goal of the ADNI has been to test whether serial magnetic resonance imaging (MRI), positron emission tomography (PET), other biological markers, and clinical and neuropsychological assessment can be combined to measure the progression of MCI and early AD. It contains data of a large number of cognitive normal, MCI, and AD subjects recruited from over 50 different centres in the US and Canada, with follow-up assessments performed every 6 months. Institutional review boards approved study procedures across participating institutions. Written informed consent was obtained from all participants.

This study considered the data of 898 participants, comprising 152 patients with AD (at baseline; same hereinafter), 474 MCI participants, and 272 cognitively normal (CN) participants. All participants had cerebrospinal fluid (CSF) biomarker data, structural MRI data, apolipoprotein E (*APOE*) genotype data, and age at examination. These variables were basically used in a previous study, which performed a hierarchical clustering of MCI participants [10]. The patients with AD and the MCI participants were diagnosed mainly by neuropsychological tests (Mini–Mental State Examination (MMSE), Clinical Dementia Rating-Sum of Boxes (CDR-SB), and Wechsler Memory Scale Logical Memory II. For this study, we used a subset of the ADNI dataset called ADNIMERGE. Table 1 shows the summary of each group.

Table 1 – The summary of samples

	CN	MCI	AD
#Subjects	272	474	152
Age (y/o)	73.9±5.8	71.9±7.4	73.9±8.3
Gender (M:F)	132:140	277:197	83:69
Edulation years	16.3±2.7	16.0±2.8	15.5±2.6

CSF biomarkers

The CSF biomarkers comprised the following five markers: Aβ (1-42) peptide levels, total tau (tTau) protein levels, phosphorylated tau (pTau) protein levels, tTau/Aβ (1-42) ratio, and pTau/Aβ (1-42) ratio. The levels of Aβ (1-42), tTau, and pTau were analysed by Roche Elecsys® immunoassays. The tTau/Aβ (1-42) ratio and pTau/Aβ (1-42) ratio were calculated by the levels of the above three CSF biomarkers. CSF biomarkers are quantitative variables but often represented by a string containing an inequality sign when the biomarker levels reached a ceiling or below the detection limit in immunoassays. Here, we treated ">1700" for Aβ (1-42) as 1,700 pg/mL and ">1300" for tTau as 1,300 pg/mL. Similarly, "<8" and ">120" for pTau were transformed into 8 pg/mL and 120 pg/mL, respectively.

Structural MRI

Structural MRI was used to determine the following five markers: whole brain volumes, ventricle volumes, hippocampus volumes, entorhinal cortex volumes, and white matter hyperintensity (WMH) volumes. These volumes were normalized as fractions of the intracranial volume (ICV). Cortical reconstruction and volumetric segmentation were performed with the FreeSurfer image analysis suite. WMHs were calculated based on coregistered T1-, T2-, and proton density (PD)-weighted structural MRI images.

***APOE* genotype**

APOE genotyping was analysed from DNA samples of each participant's blood cells using an *APOE* genotyping kit. *APOE* includes 3 alleles (ε2, ε3, ε4) and 6 genotypes (ε22, ε23, ε24,

ε33, ε34, ε44). We used the number of ε4 alleles, which is known as a risk factor for AD.

Test performance

We used the dataset from the patients with AD and the CN participants as training data to determine a decision tree and model parameters by HML. The dataset from the MCI participants was used as test data. A decision tree model generated from the training data classified the MCI participants into patients with AD (the predicted ADs) or CN participants (the predicted CNs). For test performance, the predicted ADs who converted to AD within three years were defined as true positives (*TP*). The predicted ADs who did not convert were defined as false positives (*FP*). In the same way, the predicted CNs who converted to AD within three years and those who did not convert were defined as false negatives (*FN*) and true negatives (*TN*), respectively. We calculated sensitivity, specificity, precision, and accuracy using the four outcomes as follows:

$$Sensitivity = TP / (FN + FP)$$

$$Specificity = TN / (FP + TN)$$

$$Precision = TP / (TP + FP)$$

$$Accuracy = (TP + TN) / (TP + FP + TN + FN)$$

The AD conversion in each MCI participant is presented as time-to-event data that is the number of days from age at baseline to age at onset. In this study, we defined the MCI participants who did not convert within three years as censoring data. The log-rank test was performed to evaluate the difference in conversion between the predicted ADs and the predicted CNs.

Strength of exacerbation in each variable

Linear regression analysis was used to examine the speed of temporal change in each variable in each MCI subtype separately, controlling for gender and total years of education as follows: $y = \beta_0 + \beta_{Month} \cdot Month + \beta_{Gender} \cdot Gender + \beta_{Education} \cdot Education + \varepsilon$, where y indicates the variable (*e.g.*, CSF Aβ (1-42)), β indicates the regression coefficients, and ε is the residual. The term *Month* is the total months from baseline. Intuitively, β_{Month} shows the speed of increasing (when β_{Month} is positive) or decreasing (when β_{Month} is negative) the levels of each variable. We then calculated sign-modified standardized regression coefficients to express the strength of exacerbation of each variable across three years using β_{Month}. The standardized regression coefficients were obtained from linear regression analysis after transforming all variables into Z-scores. We changed the sign of standardized regression coefficients to positive when a negative coefficient represented the exacerbation of symptoms.

Results

Test performance of a decision tree model

We inputted 152 patients with AD and 272 CN participants as training data for HML and generated the decision tree models. To explore optimal parameters, we tried four depths of decision trees and generated 30 models that were estimated by different initial values in the EM algorithm with settings at each depth (see Materials and Methods). We next applied the data from 474 MCI participants as the test data to the 120 models (= 4 depths × 30 models). The decision tree model that showed the best accuracy of all 120 models showed a sensitivity of 0.766, a specificity of 0.754, a precision of 0.568, and an accuracy of 0.757. This model was composed of seven gating nodes and eight experts (Figure 2). The performances of each expert are shown in Table 2. We also calculated the performances using single variables. As a result, the accuracy was highest with the pTau/Aβ (1-42) ratio, 0.719 (Table 3). These results indicated that the integration of multiple variables provided greater prediction.

This decision tree model with the best accuracy predicted the 190 of the MCI participants as AD (the predicted ADs) and 284 of the MCI participants as CN (the predicted CNs). We performed survival analysis to compare the conversion rates to AD between the predicted ADs and the predicted CNs. The predicted ADs progressed to AD over three years from baseline at a higher percentage (56.8%; 108/190) than the predicted CNs (11.6%; 33/284) (Figure 3).

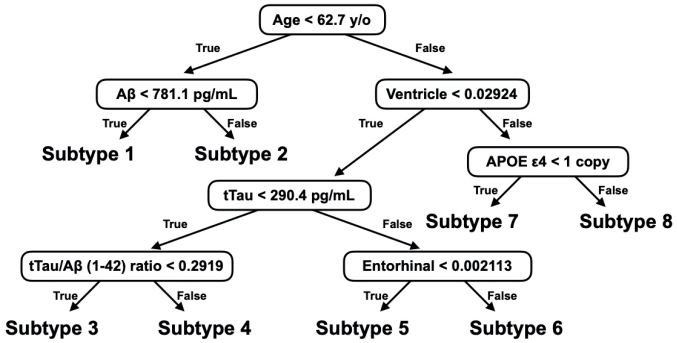

Figure 2- The decision tree model

Table 2 - Test performance of the HML algorithm.

Subtype	#Subjects	Sensitivity	Specificity	Precision	Accuracy
1	14 (2,12)	1.000	0.333	0.667	0.714
2	28 (25,3)	0.600	1.000	1.000	0.929
3	100 (94,6)	0.250	0.948	0.167	0.920
4	41 (29,12)	0.727	0.867	0.667	0.829
5	68 (6,62)	0.971	0.147	0.532	0.559
6	79 (53,26)	0.650	0.780	0.500	0.747
7	76 (60,16)	0.381	0.855	0.500	0.724
8	68 (15,53)	0.895	0.367	0.642	0.662
ALL	474 (284,190)	0.766	0.754	0.568	0.757

The numbers shown in parentheses are the number of subjects in the predicted CN and AD.

Table 3 - Test performance base on single variables.

Variable	Sensitivity	Specificity	Precision	Accuracy
Aβ (1-42)	0.662	0.722	0.497	0.705
tTau	0.446	0.776	0.453	0.679
pTau	0.496	0.758	0.460	0.681
tTau/Aβ (1-42)	0.669	0.737	0.514	0.717
pTau/Aβ (1-42)	0.662	0.743	0.517	0.719
Ventricles	0.266	0.842	0.411	0.673
Hippocampus	0.604	0.740	0.491	0.700
WholeBrain	0.475	0.797	0.493	0.703
Entorhinal	0.626	0.743	0.503	0.709
WMH	0.000	1.000	0.000	0.707
Age	0.000	1.000	0.000	0.707
APOE ε4	0.683	0.576	0.401	0.608

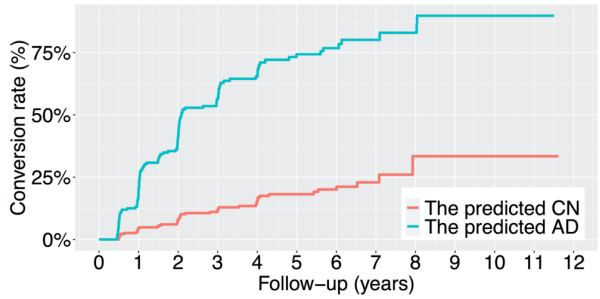

Figure 3- Conversion rates from MCI to AD in the predicted CNs (red) and the predicted ADs (green) over the measurement period. The Kaplan–Meier curves show the conversion patterns in all the MCI participants (the predicted ADs, 190 individuals; the predicted CNs, 284 individuals; p = 2.69e-29 in the log-rank test).

The characteristics in each subtype

The individuals included in an expert on a decision tree are a group of individuals with similar features. We then considered the MCI participants who were classified into a specific expert as one subtype. The MCI participants were divided as follows: 14 participants in subtype 1; 28 in subtype 2; 100 in subtype 3; 41 in subtype 4; 68 in subtype 5; 79 in subtype 6; 76 in subtype 7; and 68 in subtype 8. We compared the conversion rates of the MCI participants to AD in each subtype to characterize each subtype (Figure 4A). The Kaplan–Meier curves showed different conversion patterns in each subtype. Half or more of the MCI participants in subtypes 1, 5, and 8 progressed to AD within three years (Figure 4B). On the other hand, the conversion rates in subtypes 4, 6, and 7 were moderate, more than 25%. Subtypes 2 and 3 had comparatively low conversion rates.

To provide a more detailed characterization of each subtype, we compared the levels of the 12 variables among the subtypes (Figure 5). Subtypes 2 and 3 showed high levels of CSF Aβ (1-42) (Figure 5A), suggesting low aggregation of Aβ in the brain. The levels of CSF tau (CSF tTau, CSF pTau, tTau/Aβ (1-42) ratio, and pTau/Aβ (1-42) ratio), which indicate the degree of neuronal death in tauopathy, were high in subtypes 5 and 6 (Figure 5B-E), consistent with the structure of the decision tree. Interestingly, although subtype 1 did not have upstream gating nodes associated with tau on the decision tree, the levels of tau were high. Subtypes 7 and 8 had high ventricle volumes, suggesting brain atrophy (Figure 5F). These subtypes also had low levels of the hippocampus and whole brain volumes in accordance with enlargement of the ventricles (Figure 5G, H). Low level of the entorhinal cortex volumes was observed in subtypes 5 and 8 (Figure 5I). Regarding WMH volumes that reflect white matter lesions by cerebral ischaemia, there were no differences among the sub types (Figure 5J), implying that most MCI participants in this study did not present with vascular dementia. The top gating node in the decision tree stratified the MCI participants by age. Therefore, subtypes 1 and 2 included younger MCI participants than the other subtypes (Figure 5K). Not surprisingly, the MCI participants in subtype 7 did not have *APOE* ε4 alleles, which is a genetic risk factor, and all of the participants in subtype 8 had one or more *APOE* ε4 alleles because subtypes 7 and 8 had a gating node with *APOE* ε4 alleles (Figure 5L). On the other hand, many of those in subtype 3 did not have *APOE* ε4 alleles regardless of the absence of a gating node with *APOE* ε4 alleles, likely explaining the low conversion rate of subtype 3.

The spot matrix in Figure 6 more clearly visualizes the difference among the subtypes. Most of those in subtype 1 demonstrated both Aβ and tau abnormalities in the CSF biomarkers. There were no abnormal features in subtypes 2 and 3. Subtypes 4, 6, and 7 showed similar characteristics to the AD patients in CSF Aβ (1-42), CSF tau, and whole brain volumes, respectively. Subtypes 5 and 8 had abnormalities in CSF biomarkers and some brain atrophy. They were most severe among the subtypes, consistent with the high conversion rate shown in Figure 4.

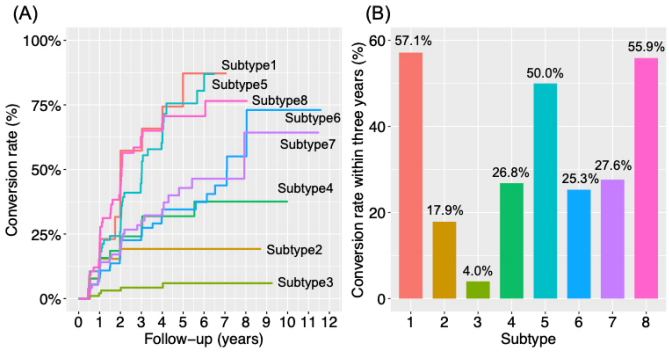

Figure 4- Conversion in each subtype. (A) The Kaplan–Meier curves in each subtype (p = 2.30e-34 in the log-rank test). (B) The conversion rate within three years in each subtype.

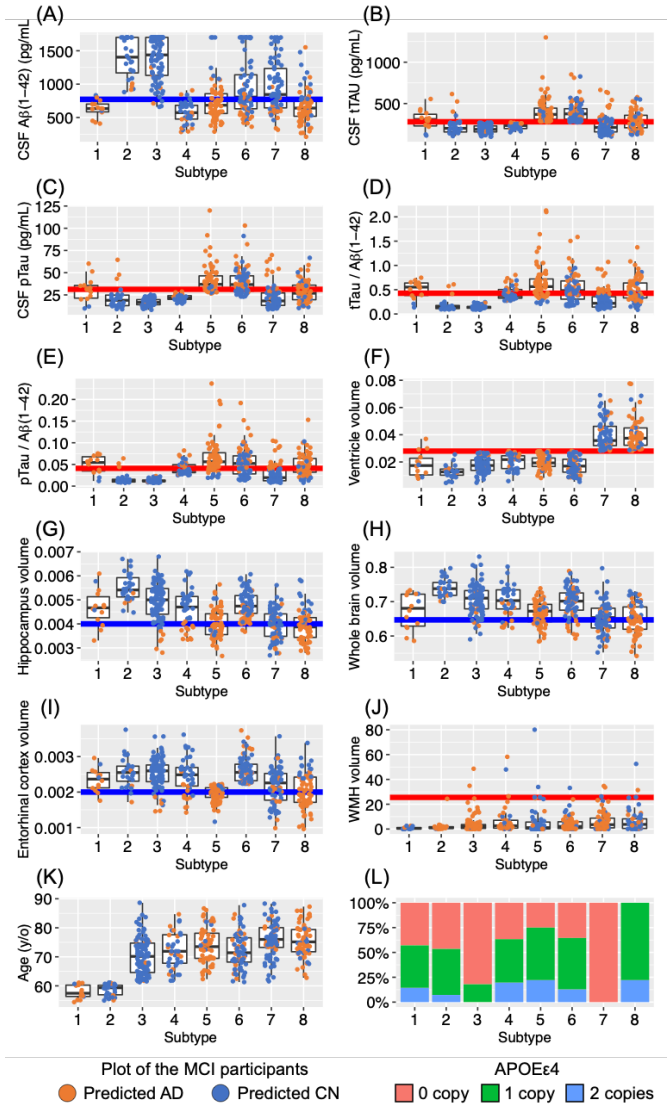

Figure 5- Features in each subtype: (A) CSF Aβ (1-42), (B) CSF tTau, (C) CSF pTau, (D) tTau/Aβ (1-42) ratio, (E) pTau/Aβ (1-42) ratio, (F) normalized ventricle volume, (G) normalized hippocampus volume, (H) normalized whole brain volume, (I) normalized entorhinal cortex volume, (J) normalized WMH volume, (K) age, and (L) APOE. Orange and blue dots represent the predicted ADs and CNs, respectively. Blue and red lines indicate the cutoff values based on the CN participants and the AD patients. Plots below a blue line or above a red line represent levels similar to the AD patients.

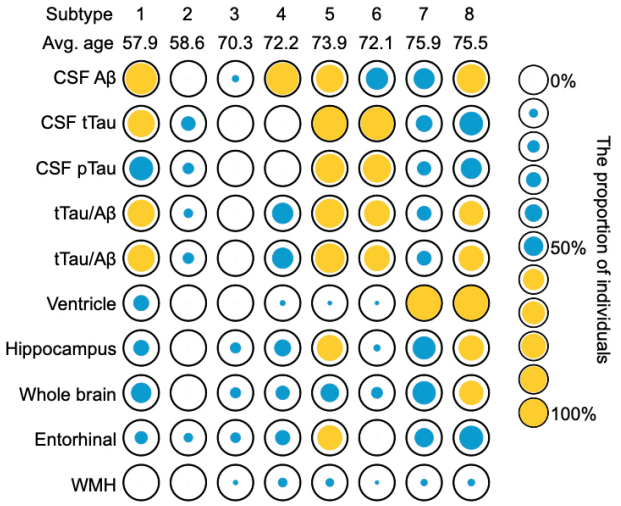

Figure 6- Spot plot showing the proportion of individuals with features similar to AD patients. Spot size represents the proportion of individuals who exceeded the cutoff value. Yellow spots indicate more than 50%.

Trajectory analysis

Finally, we examined the trajectories of the five CSF biomarkers and the four brain volumes over three years and compared the strength of exacerbation in each feature in each subtype (see Materials and Methods). Of the 474 MCI participants, 354 (74.7%) were followed for three years in the ADNI. In this analysis, subtypes 1 and 4 showed prominent exacerbation in the CSF biomarkers, specifically CSF tau (Figure 7A). Rapid exacerbation of the CSF biomarkers in subtype 1 may relate to the high conversion rate shown in Figure 4. Although subtype 4 also showed rapid exacerbation in CSF biomarkers, the conversion rate was moderate, suggesting that some of the subtype 4 progressed to other forms of dementia and not AD. The CSF biomarkers in subtype 5 were stable for three years. The levels of CSF Aβ (1-42) and tau in subtype 5 may have sufficiently reached the levels observed in AD because most of those in subtype 5 showed abnormalities of Aβ (1-42) and tau at baseline (Figures 5A-E and 6). On the other hand, progressions in atrophy of all brain regions were observed (Figure 7B). This fact confirmed the high conversion of subtype 5 (Figure 4). Typical AD first shows abnormalities in CSF Aβ (1-42) and tau that subsequently leads to brain atrophy [10]. Therefore, it would appear that subtype 5 includes MCI participants who were likely to convert to typical AD. The strength of exacerbation of brain volume measures in subtypes 2 and 3 was low, consistent with low conversion rates (Figure 4).

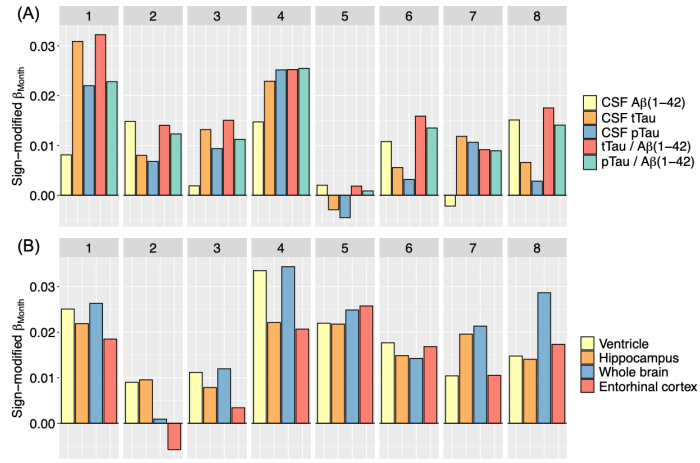

Figure 7- The strength of exacerbation of CSF biomarker abnormalities (A) and brain atrophy (B) across three years. Positive and negative coefficients indicate exacerbation and remission, respectively.

Discussion

We constructed a decision tree model to predict the conversion of MCI to AD within three years via the HML approach. The decision tree model from HML, which integrates multiple prediction models for different MCI groups derived based on the characteristics of that data, presented a higher level of accuracy than models using single variables. Additionally, we identified various subtypes of MCI based on the MCI subgroups classified by HML. The identification of these subtypes revealed varying conversion rates to AD, as well as differing levels of CSF biomarkers and brain atrophy. The MCI participants were mainly categorized into three groups in terms of AD conversion: subtypes similar to CN participants with low conversion rates (subtypes 2 and 3); subtypes with intermediate conversion rates and with any one of CSF Aβ abnormalities, CSF tau abnormalities, or brain atrophy (subtypes 4, 6, and 7); and subtypes similar to AD with high conversion rates (subtypes 1, 5, and 8).

Among the three subtypes with high conversion rates, subtypes 5 and 8 showed both CSF biomarker abnormalities and brain atrophy. On the other hand, subtype 1 had abnormalities of CSF Aβ (1-42) and tau, whereas it did not show pronounced brain atrophy. One difference between these subtypes was that the average age of subtype 1 was relatively young, 57.9 years old (Figure 5K and 6). Furthermore, the trajectory analysis across three years exhibited a rapid worsening of CSF biomarkers and brain atrophy in subtype 1, suggesting that early abnormalities in CSF biomarkers led to a more rapid progression of pathology.

The three subtypes with intermediate conversion rates were likely associated with mixed pathologies. Subtype 4 had an abnormality of CSF Aβ (1-42) at baseline (Figures 5A and 6) and subsequently showed increased tau levels (Figure 7A). These tendencies coincided with observations that changes in CSF Aβ (1-42) typically precede CSF tau abnormalities, followed by neurodegeneration and cognitive decline [11]. Subtype 6 presented abnormalities in CSF tau, although CSF Aβ (1-42) was nearly normal. The trajectory analysis also did not show increasing CSF Aβ (1-42). Subtype 6 may have included MCI participants with suspected non-Alzheimer disease pathophysiology (SNAP) that is marked by neurodegeneration without Aβ deposition within the brain [12]. The tTau is used as a biomarker for neurodegeneration [13]. However, the tau levels in our study were measured only in CSF. To further elucidate these factors, we need to incorporate measurements reflecting tau accumulation within the brain, such as tau PET. Subtype 7 was characterized by enlargement of the ventricles without CSF biomarker abnormalities. Additionally, the MCI participants in subtype 7 did not have one or more *APOE* ε4 alleles that are known to be strong genetic risk factors for AD. In the AT(N) system for classifying AD, where A is amyloid, T is tau, and N is neurodegeneration [13], these MCI participants corresponded to A-T-N+ and were consistent with non-AD pathologic changes. One of the pathologies of non-AD pathologic changes, such as A-T-N+, that can be considered is limbic-predominant age-related TDP-43 encephalopathy (LATE) [14]. The stratification of participants with MCI using biomarkers for other neurodegenerative diseases, including TDP-43 protein, would provide clarity regarding the heterogeneity of MCI.

Conclusion

In this study, we demonstrated that HML is useful for the classification of MCI participants. Our study found some subtypes similar to typical AD and identified subtypes likely to convert to other neurodegenerative diseases. These findings imply that adding other pathological information can more precisely predict the onset or progression of a wide variety of neurodegenerative diseases. Moreover, we developed the decision tree model to predict conversion to AD. Although there is room for improvement in overall performances, focusing on specific subtypes that can predict conversion to AD more accurately (*e.g.*, subtype 2 with high precision) and targeting those with MCI that were classified as AD by the prediction model of that subtype (*i.e.*, the predicted ADs) could enable more efficient clinical trials.

Acknowledgments

We acknowledge all groups that have contributed. Data collection and sharing for this project was funded by the Alzheimer's Disease Neuroimaging Initiative (ADNI) (National Institutes of Health Grant U01 AG024904).

Compliance with Ethical Standards

Department of Genome Informatics is endowed department supported by NEC Corporation. The funder (NEC Corporation) provided support in the form of salaries for authors (M.K.) but did not have any additional role in the data collection, decision to publish, or preparation of the manuscript. All other authors declare no competing interests. The study was approved by the Research Ethics Committee of Osaka University.

References

[1] World Alzheimer Report 2015: The Global Impact of Dementia.[https://www.alz.co.uk/research/world-report-2015]

[2] Cummings J, Lee G, Ritter A, Sabbagh M, Zhong K. Alzheimer's disease drug development pipeline: 2019. *Alzheimers Dement.* 2019;5:272-93.

[3] Petersen RC, Morris JC. Mild cognitive impairment as a clinical entity and treatment target. *Arch Neurol.* 2005;62(7):1160-3.

[4] Farias ST, Mungas D, Reed BR, Harvey D, DeCarli C. Progression of mild cognitive impairment to dementia in clinic- vs community-based cohorts. *Arch Neurol.* 2009;66(9):1151-7.

[5] Machulda MM, Lundt ES, Albertson SM, Kremers WK, Mielke MM, Knopman DS, Bondi MW, and Petersen RC. Neuropsychological subtypes of incident mild cognitive impairment in the Mayo Clinic Study of Aging. *Alzheimers Dement.* 2019;15(7):878-87.

[6] Blanken AE, Jang JY, Ho JK, Edmonds EC, Han SD, Bangen KJ, and Nation DA. Distilling Heterogeneity of Mild Cognitive Impairment in the National Alzheimer Coordinating Center Database Using Latent Profile Analysis. *JAMA Netw Open.* 2020;3(3):e200413.

[7] Jordan MI, Jacobs RA. Hierarchical Mixtures of Experts and the Em Algorithm. *Neural Comput.* 1994;6(2):181-214.

[8] Eto R, Fujimaki R, Morinaga S, Tamano H. Fully-Automatic Bayesian Piecewise Sparse Linear Models. *in AISTATS.* 2014;33:238-46.

[9] Mueller SG, Weiner MW, Thal LJ, Petersen RC, Jack C, Jagust W, Trojanowski JQ, Toga AW, and Beckett L. The Alzheimer's disease neuroimaging initiative. *Neuroimaging Clin N Am.* 2005;15(4):869-77.

[10] Nettiksimmons J, DeCarli C, Landau S, Beckett L, for the Alzheimer's Disease Neuroimaging Initiative. Biological heterogeneity in ADNI amnestic MCI. *Alzheimers Dement.* 2014;10(5): 511–521.e1.

[11] Jack CR, Jr., Knopman DS, Jagust WJ, Petersen RC, Weiner MW, Aisen PS, Shaw LM, Vemuri P, Wiste HJ, Weigand SD, Lesnick TG, Pankratz VS, Donohue MC, and Trojanowski JQ. Tracking pathophysiological processes in Alzheimer's disease: an updated hypothetical model of dynamic biomarkers. *Lancet Neurol.* 2013;12(2):207-16.

[12] Jack CR, Jr., Knopman DS, Weigand SD, Wiste HJ, Vemuri P, Lowe V, Kantarci K, Gunter JL, Senjem ML, Ivnik RJ, Roberts RO, Rocca WA, Boeve BF, Petersen RC. An operational approach to National Institute on Aging-Alzheimer's Association criteria for preclinical Alzheimer disease. *Ann Neurol.* 2012;71(6):765-75.

[13] Jack CR, Jr., Bennett DA, Blennow K, Carrillo MC, Feldman HH, Frisoni GB, Hampel H, Jagust WJ, Johnson KA, Knopman DS, Petersen RC, Scheltens P, Sperling RA, and Dubois B. A/T/N: An unbiased descriptive classification scheme for Alzheimer disease biomarkers. *Neurology.* 2016;87(5):539-47.

[14] Nelson PT, Dickson DW, Trojanowski JQ, Jack CR, Boyle PA, Arfanakis K, Rademakers R, Alafuzoff I, Attems J, Brayne C, Coyle-Gilchrist ITS, Chui HC, Fardo DW, Flanagan ME, Halliday G, Hokkanen SRK, Hunter S, Jicha GA, Katsumata Y, Kawas CH, Keene CD, Kovacs GG, Kukull WA, Levey AI, Makkinejad N, Montine TJ, Murayama S, Murray ME, Nag S, Rissman RA, Seeley WW, Sperling RA, White Iii CL, Yu L, and Schneider JA. Limbic-predominant age-related TDP-43 encephalopathy (LATE): consensus working group report. *Brain.* 2019;142(6):1503-27.

Address for correspondence

Masataka Kikuchi

2-2 Yamadaoka, Suita, Osaka 565-0871, Japan

Phone No.: +81-6-6210-8361

Fax No.: +81-6-6210-8365

Email Address: kikuchi@gi.med.osaka-u.ac.jp